Journal of Coordination Chemistry

ISSN: 0095-8972 (Print) 1029-0389 (Online) Journal homepage: http://www.tandfonline.com/loi/gcoo20

Synthesis, structures, catalytic, and anticancer activities of some coordination compounds involving two new triazole derivatives

Dan Xiao, Ying-Hui Yu, Zi-Shi Wang, Chun-Hui Yu, Guang-Feng Hou, Yan-Mei Chen, Xian-Feng Gong, Dong-Sheng Ma & Jin-Sheng Gao

To cite this article: Dan Xiao, Ying-Hui Yu, Zi-Shi Wang, Chun-Hui Yu, Guang-Feng Hou, Yan-Mei Chen, Xian-Feng Gong, Dong-Sheng Ma & Jin-Sheng Gao (2015) Synthesis, structures, catalytic, and anticancer activities of some coordination compounds involving two new triazole derivatives, Journal of Coordination Chemistry, 68:13, 2225-2239, DOI: 10.1080/00958972.2015.1042375

To link to this article: http://dx.doi.org/10.1080/00958972.2015.1042375

Journal of Coordination Chemistry, 2015
Vol. 68, No. 13, 2225–2239, http://dx.doi.org/10.1080/00958972.2015.1042375

Synthesis, structures, catalytic, and anticancer activities of some coordination compounds involving two new triazole derivatives

DAN XIAO†, YING-HUI YU†, ZI-SHI WANG‡, CHUN-HUI YU†, GUANG-FENG HOU*†‡, YAN-MEI CHEN†, XIAN-FENG GONG†, DONG-SHENG MA*† and JIN-SHENG GAO†‡

†School of Chemistry and Materials Science, Heilongjiang University, Harbin, China
‡Engineering Research Center of Pesticide of Heilongjiang University, Heilongjiang University, Harbin, China

(*Received 2 November 2014; accepted 26 March 2015*)

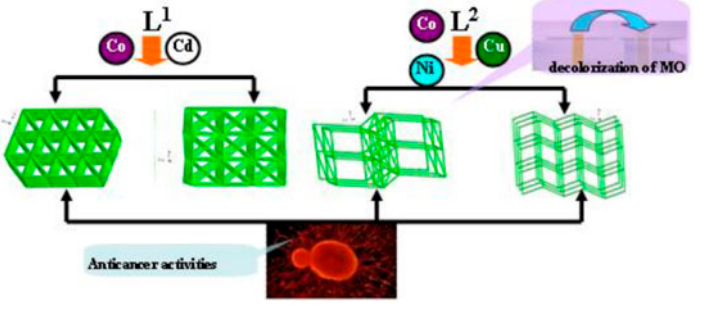

Five N-heterocyclic carboxylate based coordination complexes are synthesized which all show hydrogen bonding supramolecular structures, and the photocatalytic and anticancer activities of them are investigated.

Five N-heterocyclic carboxylate-based coordination complexes, $[Co(L^1)_2(H_2O)_2]\cdot 2H_2O$ (**1**), $[Cd(L^1)_2(H_2O)_2]\cdot 2H_2O$ (**2**), $[Co(L^2)(H_2O)_3]$ (**3**), $[Ni(L^2)(H_2O)_3]$ (**4**), and $[Cu_2(L^2)_2(H_2O)_2]$ (**5**), have been synthesized and characterized by elemental analysis, IR spectroscopy, Powder X-ray diffraction, thermogravimetric analyses, and single-crystal X-ray crystallography, where HL^1 is 2-((5-amino-1H-1,2,4-triazol-3-yl)thio)acetic acid and H_2L^2 is 2-((5-amino-1-(carboxymethyl)-1H-1,2,4-triazol-3-yl) thio)acetic acid. In these complexes, the hydrogen bonds (H-bonds) play an important role in their packing structures. Complex **1** has nine H-bonds showing a 3-D *sqc38* topology. Complex **2** has 17 H-bonds exhibiting a 3-D *hxl* network. Complexes **3** and **4** are isomorphic, both of which possess ten H-bonds to present a 3-D *btc* topology. Complex **5** with eight H-bonds forms a 2-D *sq1* structure. In addition, complex **3** catalyzes the decolorization of methyl orange. Meanwhile, **1**, **3**, and **5** show certain anticancer activities to inhibit the growth of HepG2 cells.

Keywords: Crystal structure; Triazole; Hydrogen bond; Catalytic property

*Corresponding authors. Email: hougf@hlju.edu.cn (G.-F. Hou); 1986011@hlju.edu.cn (D.-S. Ma)

1. Introduction

Construction of nitrogen-containing heterocycles (N-heterocycles) has attracted significant interest owing to their enormous structural diversity and intriguing molecular topologies as well as promising applications as functional materials in catalysis, sorption, ion exchange, sensors, nonlinear optics, magnetism, etc. [1–3]. It is well-known that some simple N-heterocyclic ligands, such as pyridine, imidazole, pyrazine, and triazole, could be easily obtained and modified. Therefore, decoration of carboxylic acid groups to these N-heterocycles has become a simple and effective approach to prepare multidentate ligands. As multidentate ligands, the obtained N-heterocyclic carboxylates possess both oxygen and nitrogen donors, which can coordinate with metal ions [4–6]; pyridine-2,n-dicarboxylic acids (n = 3, 5, 6) (scheme S1, see online supplemental material at http://dx.doi.org/10.1080/00958972.2015.1042375) are examples. Several examples have been reported including 3d–4f heterometallic coordination complexes as selective luminescent probes [7–12].

In addition to six-membered N-heterocycles, five-membered rings such as imidazole, triazole, etc. can also be modified by carboxylic acid groups to construct new ligands, however, the reports of which are relatively few. In 2007, Du *et al.* found that reaction of 2-(4-pyridyl)thiazole-4-carboxylic acid (Hptca) (scheme S1) with different divalent metal ions could lead to diverse metal-organic supramolecular architectures in different dimensions [13]. In 2012, Hou *et al.* reported a series of coordination complexes based on 2-((1H-1,2,4-triazol-1-yl)methyl)-1H-imidazole-4,5-dicarboxylic acid (H_3tmidc) (scheme S1) exhibiting unique structures and excellent magnetic properties [14]. Triazole and its derivatives usually have good biological activities [15, 16], which could be maintained in their coordination complexes [17]. However, reports of the biological activities of triazole complexes are still limited. Some N-heterocyclic carboxylate ligands reported in recent years are listed in scheme S1.

We present here two N-heterocyclic carboxylate ligands, 2-((5-amino-1H-1,2,4-triazol3-yl)thio)acetic acid (HL^1) and 2-((5-amino-1-(carboxymethyl)-1H-1,2,4-triazol-3-yl)thio) acetic acid (H_2L^2), which are synthesized from 5-amino-1H-1,2,4-triazole-3-thiol with chloroacetic acid. The amino- and mercapto-groups are introduced into the triazole ring considering the following points: (a) the existence of $–NH_2$, $–NO_2$, and –OH groups could enhance the performance of the triazole derivatives in biological activities and gas adsorption properties [18–21] and (b) the $–NH_2$ and –SH groups can be easily further decorated with carboxylate and other functional groups [22]. Five complexes are constructed by HL^1 or H_2L^2 reacting with transition metals in different conditions: $[Co(L^1)_2(H_2O)_2]\cdot 2H_2O$ (**1**), $[Cd(L^1)_2(H_2O)_2]\cdot 2H_2O$ (**2**), $[Co(L^2)(H_2O)_3]$ (**3**), $[Ni(L^2)(H_2O)_3]$ (**4**), and $[Cu_2(L^2)_2(H_2O)_2]$ (**5**). Noticeably, there are abundant hydrogen bonds (H-bonds) in these complexes. Though hydrogen bonds are not normally as strong as coordinate bonds, their combined influence can make a huge impact on the resulting network [23–26], due to the fact that complementary H-bonding interactions contribute significantly to shaping the hierarchical supramolecular structure. When a metal-organic complex is formed, the noncoordinated nitrogen donor sites can H-bond forming a supramolecular structure [27]. These five complexes with free $–NH_2$ groups, uncoordinated N of triazole, and the crystallization water molecules are good candidates for constructing supramolecular architectures (scheme 1).

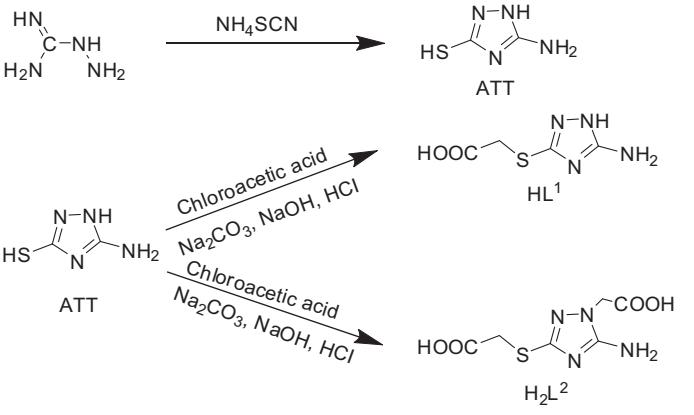

Scheme 1. The synthetic route of HL^1 and H_2L^2.

2. Experimental

2.1. *Materials and method*

All solvents and reagents for the syntheses were commercially available and used as received. Elemental analyses were performed on a PerkinElmer-2400 Series II analyzer. IR spectra were recorded on a PerkinElmer precisely Spectrum 100 apparatus from 450 to 4000 cm^{-1}. The dry sample powder is mixed with KBr for IR spectra. The ^{1}H-NMR spectra were recorded on a Bruker 400 MHz NMR spectrometer (USA) using DMSO as a solvent. Powder X-ray diffraction (PXRD) measurements were performed on a Bruker D8 Advance X-ray diffractometer using Cu-Kα radiation (λ = 1.5418 Å), in which the X-ray tube was operated at 40 kV and 40 mA at room temperature and compared to simulated patterns. The UV–vis spectra were recorded on a PerkinElmer lambda 25 using distilled water as a solvent. Thermogravimetric measurements were performed on a PerkinElmer TGA 7 analyzer.

2.2. *Preparation of HL^1 and H_2L^2*

HL^1 and H_2L^2 were prepared from the same reactants, 5-amino-1H-1,2,4-triazole-3-thiol and 2-chloroacetic acid under different molar ratio and reaction conditions.

Step 1: A mixture of aminoguanidine bicarbonate (27.78 g, 0.2 mol), ammonium thiocyanate (8.27 g, 0.24 mol), and 10 mL of distilled water was added into a 250-mL three-necked flask equipped with a motor stirrer, a thermometer, and a tail gas absorption device. The resulting solution was heated to 80 °C under stirring until no air bubbles were observed, and the produced water was then removed by vacuum distillation. Concentrated hydrochloric acid (27.6 mL) was added dropwise to the above mixture and kept stirring for 1 h. After that, 22 mL aqueous solution (40%) of NaOH was added dropwise, and the resulting solution was heated and refluxed for 2 h, which was then cooled to room temperature. The white gray crude product was obtained by filtration after the pH was adjusted to 1 by concentrated hydrochloric acid. Recrystallization of the crude product from water gives white pure 5-amino-1H-1,2,4-triazole-3-thiol (ATT) with a yield of 80.1%. ^{1}H-NMR

(400 MHz, DMSO) δ: 12.26 (s, 1H), 12.04 (s, 1H), 5.72 (s, 2H). IR (KBr, cm^{-1}): 3378(m), 1644(s), 1584(m), 1481(m), 1231(s), 1135(m), 1066(w), 1025(m). Elemental Analysis (%): Found (Calcd) for **ATT**: C, 20.72 (20.68); H, 3.45 (3.47); N, 48.22 (48.24).

Step 2: A mixture of ATT 11.6 g (0.1 mol), sodium carbonate 10.6 g (0.1 mol), and sodium hydroxide 4 g (0.1 mol) was added into 100 mL of water under stirring, and then, the reaction system was cooled to 10 °C and kept for 15 min to get a clear solution. Then, 50 mL water solution containing chloroacetic acid (11.3 g, 0.12 mol) and sodium hydroxide (4.8 g, 0.12 mol) was added dropwise [chloroacetic acid (20.8 g, 0.22 mol) and sodium hydroxide (8.8 g, 0.22 mol) were used for synthesis of H_2L^2]. The resultant solution was heated to reflux with stirring for 8 h, cooled to room temperature, and then, the pH was adjusted to about 2 with concentrated hydrochloric acid. After stirring for 20 min, the product of 2-((5-amino-1H-1,2,4-triazol-3-yl)thio)acetic acid $\mathbf{HL^1}$ with a yield of 75.2% was obtained [2-((5-amino-1-(carboxymethyl)-1H-1,2,4-triazol-3-yl)thio)acetic acid $\mathbf{H_2L^2}$ with a yield of 73.4%]. $\mathbf{HL^1}$: ^{1}H-NMR (400 MHz, DMSO) δ: 3.50 (s, 2H, CH_2). IR (KBr, cm^{-1}): 1586 (s), 1411 (s), 1281 (w), 1215 (m), 1083 (m), 897 (w). Elemental Analysis (%): Found (Calcd) for $\mathbf{HL^1}$: C, 27.45 (27.58); H, 3.52 (3.47); N, 32.25 (32.17). $\mathbf{H_2L^2}$: ^{1}H-NMR (400 MHz, DMSO) δ: 6.41 (s, 2H, CH_2), 4.57 (s, 2H, CH_2), 3.78 (s, 2H, NH_2). IR (KBr, cm^{-1}): 1730 (s), 1676 (s). Elemental Analysis (%): Found (Calcd) for $\mathbf{H_2L^2}$: C, 31.08 (31.03); H, 3.44 (3.47); N, 24.11 (24.13).

2.3. *Syntheses of 1–5*

2.3.1. Syntheses of $[Co(L^1)_2(H_2O)_2]\cdot 2H_2O$ (1). A mixture of HL^1 (0.5 mmol, 0.087 g), $CoCl_2\cdot 6H_2O$ (0.5 mmol, 0.12 g) and 5 mL distilled water was added into a 20-mL Teflon-lined autoclave and the pH adjusted to 7 by NaOH solution (4 M). The autoclave was heated at 120 °C for 72 h. After cooling slowly to room temperature, pink block crystals were obtained. Yield: 171.8 mg (72% yield based on Co). Elemental analysis (%): Found (Calcd) for $C_8H_{18}CoN_8O_8S_2$: C, 20.17 (20.13); H, 3.78 (3.80); N, 23.41 (23.48). IR (KBr, cm^{-1}): 1632 (s), 1570 (s), 1499 (s), 1400 (s), 1367 (m), 1287 (m), 1242 (s), 1116 (m), 1072 (m), 1012 (w), 939 (m), 906 (s).

2.3.2. Synthesis of $[Cd(L^1)_2(H_2O)_2]\cdot 2H_2O$ (2). The preparation of **2** was similar to that of **1** except that the $CdCl_2\cdot 2.5H_2O$ (0.5 mmol, 0.114 g) was used instead of $CoCl_2\cdot 6H_2O$, and the pH was adjusted to 8–9. Colorless block crystals were filtered and washed with distilled water. Yield: 132.7 mg (50% yield based on Cd). Elemental analysis (%): Found (Calcd) for $C_8H_{18}CdN_8O_8S_2$: C, 18.13 (18.10); H, 3.47 (3.42); N, 21.05 (21.11). IR (KBr, cm^{-1}): 1649 (s), 1570 (s), 1494 (s), 1394 (m), 1380 (m), 1282 (m), 1249 (s), 1110 (m), 1062 (m), 1022 (w), 925 (m), 901 (m).

2.3.3. Synthesis of $[Co(L^2)(H_2O)_3]$ (3). A mixture of H_2L^2 (0.5 mmol, 0.115 g), $CoCl_2\cdot 6H_2O$ (1.5 mmol, 0.36 g), and 5 mL distilled water was added into a 20-mL Teflon-lined autoclave and the pH adjusted to 7 by NaOH solution (4 M). The autoclave was heated at 120 °C for 72 h. After slowly cooling to room temperature, purple block crystals were obtained. Yield: 324.3 mg (63% yield based on Co). Elemental analysis (%): Found (Calcd) for $C_6H_{12}CoN_4O_7S$: C, 21.03 (21.00); H, 3.49 (3.52); N, 16.31 (16.33). IR (KBr,

cm^{-1}): 1670 (m), 1581 (s), 1514 (m), 1398 (m), 1329 (s), 1272 (w), 1130 (m), 1022 (w), 948 (m), 862 (w), 729 (m), 667 (w).

2.3.4. Synthesis of $[Ni(L^2)(H_2O)_3]$ (4). The preparation of **4** was similar to that of **3** except that $Ni(CH_3COO)_2{\cdot}4H_2O$ (0.3 mmol, 0.075 g) was used instead of $CoCl_2{\cdot}6H_2O$. 39.1 mg light green diamond-shaped crystals were obtained (38% yield based on Ni). Elemental analysis (%): Found (Calcd) for $C_6H_{12}NiN_4O_7S$: C, 21.07 (21.01); H, 3.56 (3.53); N, 16.31(16.34). IR (KBr, cm^{-1}): 1669 (m), 1585 (s), 1511 (m), 1409 (m), 1322 (s), 1275 (w), 1225 (m), 1118 (m), 1019 (w), 955 (m), 854 (w), 719 (m), 661 (m).

2.3.5. Synthesis of $[Cu_2(L^2)_2(H_2O)_2]$ (5). The mixture of H_2L^2 (0.25 mmol, 0.058 g), $Cu(NO_3)_2{\cdot}3H_2O$ (0.5 mmol, 0.121 g), acetonitrile (5 mL), distilled water (5 mL), and a drop of NaOH (4 M) was kept stirring for 30 min and then filtered. The filtrate was slowly evaporated at room temperature to obtain dark green block-shaped crystals in a few days. Yield: 73.3 mg (47% yield based on Cu). Elemental analysis (%): Found (Calcd) for $C_{12}H_{16}Cu_2N_8O_{10}S_2$: C, 23.10 (23.12); H, 2.61 (2.59); N, 17.95 (17.97). IR (KBr, cm^{-1}): 1642 (s), 1564 (s), 1495 (m), 1372 (s), 1319 (m), 1258 (w), 1123 (m), 955 (w), 725 (m), 601 (m).

2.4. *X-ray crystallography*

Suitable single crystals of **1–5** were carefully selected under an optical microscope and glued to thin glass fibers. Crystallographic data for all complexes were collected with a Siemens SMART CCD diffractometer with graphite-monochromated Mo Kα radiation ($\lambda = 0.71073$ Å) at $T = 293(2)$ K. Data processing was accomplished using SAINT. The structures were solved using direct methods and refined by full-matrix least-squares on F^2 using SHELX–97 [28]. All non-hydrogen atoms were refined anisotropically. A summary of the crystallographic data and structure refinement parameters for **1–5** are given in table 1. Selected bond lengths and angles for **1–5** are given in table S1. Hydrogen bond parameters for **1–5** are given in table S2. CCDC 1015799–803 contain the supplementary crystallographic data for **1–5**.

2.5. *Decolorization of MO*

The decolorization experiment of MO is conducted in a 250-mL glass beaker. In this experiment, 50 mL MO sample with the original concentration of 15 mg L^{-1} is used and six parallel experiments conducted at the same time. All experiments were carried out under conditions of sunlight and room temperature. The concentration of MO is measured by the UV maximum absorption wavelength at 464 nm.

2.6. *Anticancer activity test for HepG2 cells*

The HepG2 cells with density of 1×10^5 cells mL^{-1} were seeded in 96-well plates and **1**, **3**, and **5** were added with the final concentration of 150 μM. After culturing for 24 h, the supernatant was taken out of the well plates and 100 μL sterilized 0.9% sodium chloride

Table 1. Crystallographic data for the structural analyses of **1–5**.

Complex	**1**	**2**	**3**	**4**	**5**
Chemical formula	$C_8H_{18}CoN_8O_8S_2$	$C_8H_{18}CdN_8O_8S_2$	$C_6H_{12}CoN_4O_7S$	$C_6H_{12}N_4NiO_7S$	$C_{12}H_{16}Cu_2O_{10}S_2$
Formula weight	477.4	530.9	343.2	343.0	623.5
Crystal system	Monoclinic	Monoclinic	Triclinic	Triclinic	Monoclinic
Space group	$P2_1/c$	$P2_1/c$	$P\bar{1}$	$P\bar{1}$	$C2/c$
a (Å)	8.0861(3)	7.7813(4)	6.3946(6)	6.3750(5)	18.1621(9)
b (Å)	15.3851(3)	15.4890(8)	7.1621(5)	7.1299(6)	8.1692(3)
c (Å)	7.5404(3)	14.4828(7)	13.3190(10)	13.2861(11)	13.5685(6)
α (°)	90	90	98.317(6)	98.354(7)	90
β (°)	116.887(4)	91.582(5)	97.665(7)	97.821(7)	92.920(4)
γ (°)	90	90	90.484(7)	90.744(6)	90
V (Å^3)	836.66(5)	1744.87(15)	597.95(8)	591.60(8)	2010.54(15)
Crystal size (mm^3)	0.22 × 0.19 × 0.15	0.25 × 0.22 × 0.19	0.26 × 0.21 × 0.17	0.20 × 0.17 × 0.14	0.23 × 0.19 × 0.15
Z	2	4	2	2	4
D_c (mg·cm^{-3})	1.895	2.021	1.906	1.925	2.060
μ (mm^{-1})	1.337	1.551	1.647	1.854	2.398
F(0 0 0)	490	1064	350	352	1256
Reflections collected/unique	3003/1465	7017/3068	3923/2126	3798/2092	3551/1766
R_{int}	0.0205	0.0194	0.0205	0.0198	0.0238
No. of data/restraints/parameters	1465/8/145	3068/14/244	2126/11/196	2092/11/196	1766/11/171
GOF on F^2	1.068	1.090	1.056	1.069	1.023
R indices	$R_1 = 0.0254$	$R_1 = 0.0309$	$R_1 = 0.0285$	$R_1 = 0.0266$	$R_1 = 0.0331$
[$I > 2\sigma(I)$]	$wR_2 = 0.0603$	$wR_2 = 0.0798$	$wR_2 = 0.0671$	$wR_2 = 0.0588$	$wR_2 = 0.0779$
R indices (all data)	$R_1 = 0.0292$	$R_1 = 0.0357$	$R_1 = 0.0342$	$R_1 = 0.0314$	$R_1 = 0.0397$
	$wR_2 = 0.0627$	$wR_2 = 0.0830$	$wR_2 = 0.0715$	$wR_2 = 0.0616$	$wR_2 = 0.0826$
Largest diff. in peak/hole (e Å^{-3})	0.250/−0.263	0.439/−0.825	0.253/−0.299	0.305/−0.271	0.713/−0.549

solution was added to wash the well plates, and then, the supernatant was discarded again. Then, 100 μL new culture solution and 20 μL MTT (3-(4,5-dimethyl-thiazol-2)-2,5-diphenyl tetrazole bromide) dyeing liquid were added to the incubator. After 4 h, the supernatant was removed in the plates and 150 μL DMSO was added to each well and vibrated for 10 min in the micro-oscillator. The inhibition rates for HepG2 cells were calculated by the absorbance value A of the solution measured by enzyme immunoassay instrument.

$$\text{Inhibition rate}\,(\%) = \frac{A_{\text{blank}} - A_{\text{dosing group}}}{A_{\text{blank}}} \times 100\%$$

3. Results and discussion

3.1. *Crystal structure descriptions*

Complexes **1–4** were hydrothermally synthesized and **5** was obtained by volatilizing its supersaturated solution. Influence of the reaction conditions on the synthesis of **1–4** was also investigated, such as temperature, molar ratio of the reactants, solvent, pH as well as the filling degree of the autoclave. The pH value plays a key role in the formation of **1–4**.

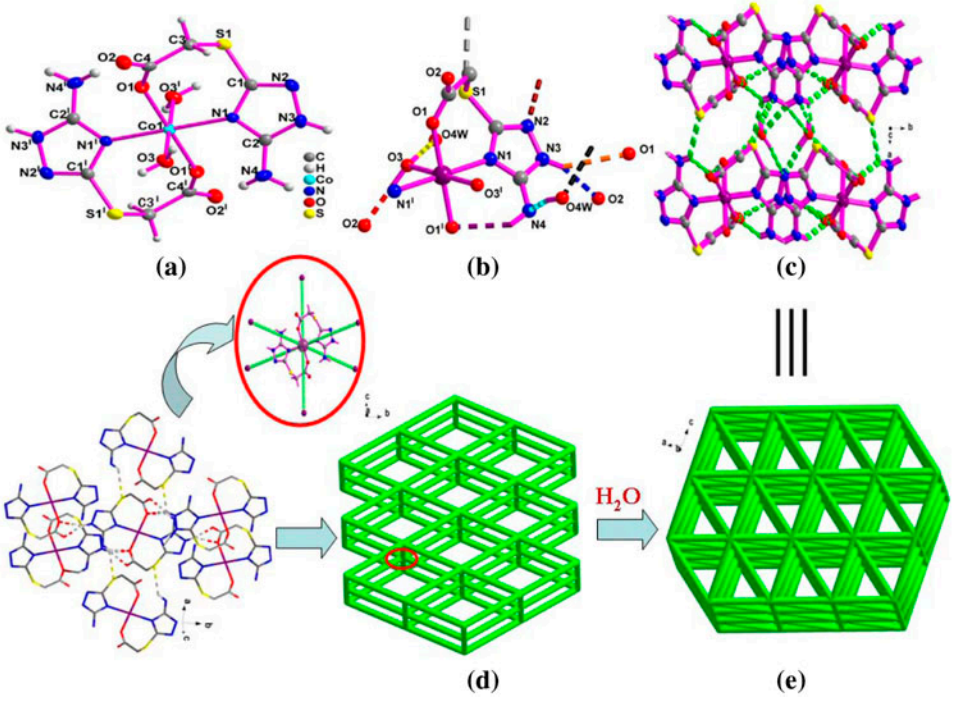

Figure 1. (a) The coordination environment of Co(II) in **1**. (b) The details of nine H-bonds in the asymmetric unit. (c) Side view of 3-D H-bonding network along the *c* axis. (d) Schematic illustration of the 3-D 6-connected *sqc1* network with a point symbol ($4^{12}\cdot6^3$) formed by H-bonds (the lattice water molecules were excluded). (e) 3-D 14-connected *sqc38* network with a point symbol of ($3^{36}\cdot4^{48}\cdot5^7$) of **1**. Symmetry code: $I = 1 - x, -y, 1 - z$.

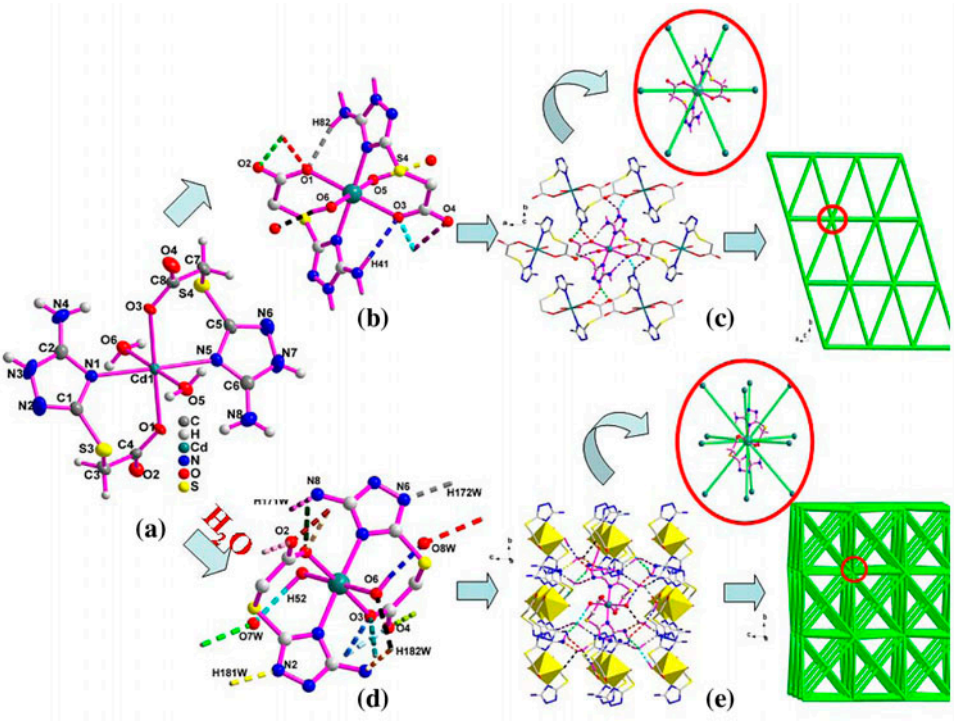

Figure 2. (a) The coordination environment of Cd(II) in **2**. (b) The details of eight H-bonds of the asymmetric unit excluding the lattice water molecules. (c) 2-D H-bonding *hxl* network with a point symbol of $(3^6{\cdot}4^6{\cdot}5^3)$. (d) 17 H-bonds of the asymmetric unit containing lattice waters. (e) 3-D 12-connected *sqc19* network with a point symbol of $(3^{24}{\cdot}4^{36}{\cdot}5^6)$.

Both L^1 and L^2 decompose when the reaction temperature is higher than 170 °C. For the synthesis of **5**, experiments were tried under other conditions, but no suitable single crystals were obtained.

Complex 1. Single-crystal X-ray analysis shows that **1** crystallized in the monoclinic system with $P2_1/c$ space group. The asymmetric unit of **1** consists of a half of Co(II), one L^1, one coordinated water, and one crystallization water. As shown in figure 1(a), Co ion is six-coordinate with slightly distorted octahedral geometry surrounded by two oxygens and two nitrogens (O1, $O1^I$, N1, and $N1^I$) from two crystallographic independent L^1 ligands and two waters (O3 and $O3^I$). The Co1–O distances are 2.101(1)–2.124(2) Å, while Co1–N bond length is 2.136(2). The angles around Co ion are 84.85(6)–180°.

In **1**, one asymmetric unit has nine H-bonds [figure 1(b)] to connect the adjacent units and lattice water molecules leading to a 3-D supramolecular structure [figure 1(c)]. When the lattice water is excluded, one $[Co(L^1)_2(H_2O)_2]$ building block would connect other six blocks to get a *sqc1* topology with a point symbol of $(4^{12}{\cdot}6^3)$ [figure 1(d)]. However, the lattice waters fill in the cavities to form H-bonds with the coordinated water, the carboxylate groups, and the uncoordinated N of L^1, which further intertwines with the *sqc1* network into a 14-connected *sqc38* network with a point symbol of $(3^{36}{\cdot}4^{48}{\cdot}5^7)$ simplified by the TOPOS program [29] [figure 1(e)].

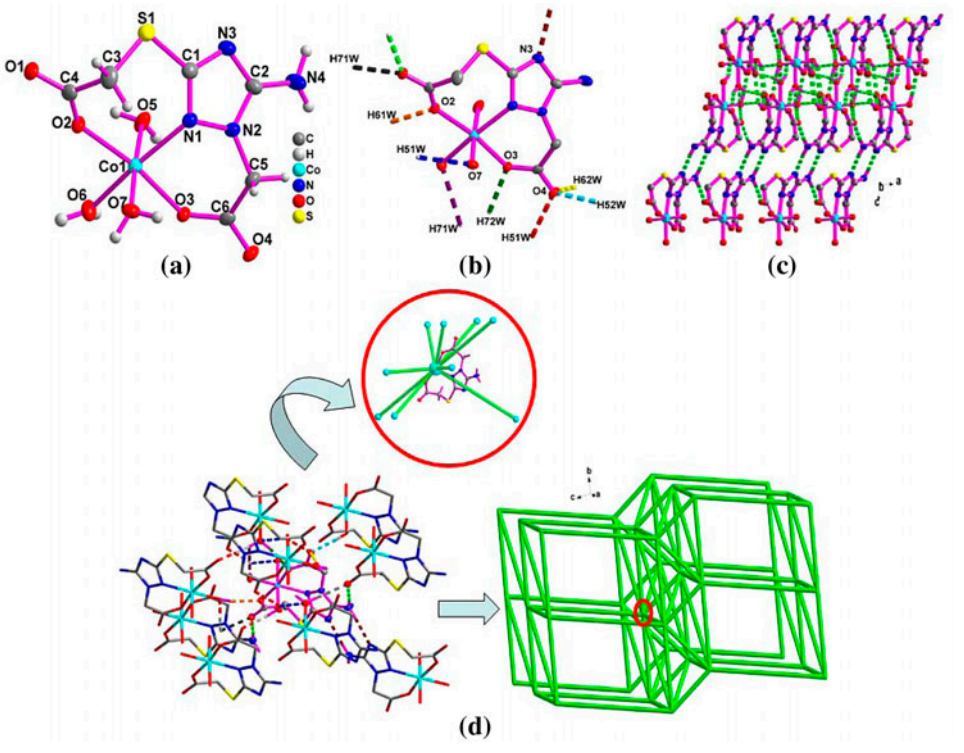

Figure 3. (a) The coordination environment of Co(II) in **3**. (b) The details of ten H-bonds. (c) 3-D structure of **3** built up by H-bonds. (d) Schematic illustration of the 3-D 9-connected *btc* network with a point symbol of $(3^9\cdot4^{19}\cdot5^8)$.

Complex 2. Complex **2** also crystallized in the monoclinic system with $P2_1/c$ space group. The asymmetric unit consists of one Cd(II), two L^1 ligands, two coordinated waters, and two lattice waters [figure 2(a)]. Cd1 is six-coordinate with slightly distorted octahedral geometry surrounded by two oxygens and two nitrogens (O1, O3, N1, and N5) from two crystallographic independent L^1 ligands and two water ligands (O5 and O6). The Cd–O distances are 2.326(3)–2.350(2) Å and the Cd–N bond lengths are 2.263(3)–2.264(3) Å. When the lattice water molecules are not considered, there are eight H-bonds in the asymmetric unit of **2** [figure 2(b)], which link another six $[Cd(L^1)_2(H_2O)_2]$ moieties to build up a 2-D 6-connected *hxl* topology with a point symbol of $(3^6\cdot4^6\cdot5^3)$ [figure 2(c)]. The lattice water molecules fill in the cavities of this *hxl* network and form H-bonds with $[Cd(L^1)_2(H_2O)_2]$ moieties. As a result, the neighboring sheets are further pillared to construct a 3-D supramolecular architecture, which can be simplified to 12-connected *sqc19* network with a point symbol of $(3^{24}\cdot4^{36}\cdot5^6)$.

Complex 3. Single-crystal X-ray analysis shows that **3** and **4** are essentially isomorphic, so only the structure of **3** is described here in detail. Complex **3** crystallized in the triclinic system with $P\bar{1}$ space group. The asymmetric unit of **3** consists of one Co(II), one L^2, and three coordinated waters [figure 3(a)]. Co1 is also six-coordinate with slightly distorted octahedral geometry, but surrounded by two oxygens and one nitrogen (O2, O3, and N1) from L^2 and three water ligands (O5, O6, and O7). In **3**, L^2 is tridentate with Co1, being

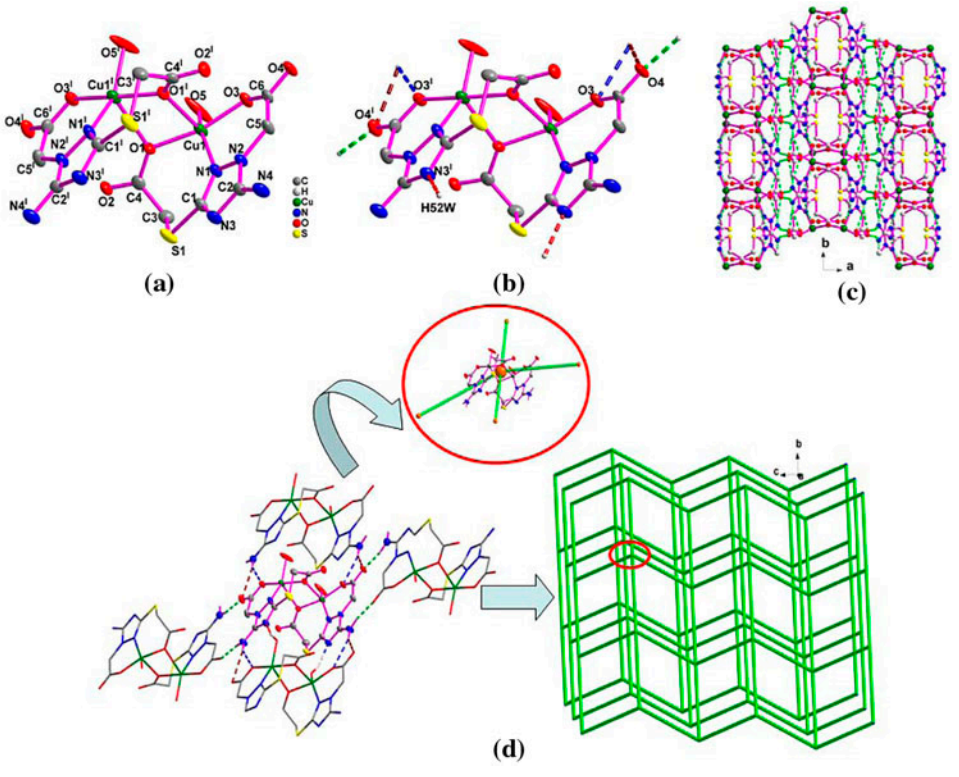

Figure 4. (a) The molecular structure of **5**. (b) The details of eight H-bonds. (c) 2-D structure of **5** formed by H-bonds. (d) Schematic illustration of the **sq1** topology of **5** with a point symbol of $(4^4{\cdot}6^2)$. Symmetry codes: $I = 1 - x, y, 1.5 - z$.

different from that of **1**, in which the L^1 is bidentate. The Co1–O distances are 2.037 (2)–2.152(2) Å and the Co1–N bond length is 2.141(2) Å, similar to those of **1**.

The crystal structure of **3** shows the self-organizing behavior of $[Co(L^2)(H_2O)_3]$ building blocks derived from a variety of H-bonds. The asymmetric unit of **3** with ten H-bonds [figure 3(b)] links adjacent nine $[Co(L^2)(H_2O)_3]$ moieties leading to a supramolecular 3-D network [figure 3(c)]. Furthermore, this network can be simplified to *btc* net structure with a point symbol of $(3^9{\cdot}4^{19}{\cdot}5^8)$, when the $[Co(L^2)(H_2O)_3]$ moieties are seen as 9-connected nodes [figure 3(d)].

Complex 5. Complex **5** also crystallized in the triclinic system with $P\bar{1}$ space group. The results of crystallographic analysis reveal that the asymmetric unit of **5** consists of one Cu (II), one L^2,and one coordinated water ligand. Figure 4(a) shows the molecular structure of **5**, in which Cu1 is five-coordinate with slightly distorted square pyramidal geometry defined by three oxygens and one nitrogen (O1, $O1^I$, O3, and N1) from one L^2 and one water (O5). The Cu1–O distances are 1.908(3)–2.323(3) Å and the Cu1–N bond length is 1.977(3) Å. Each molecule of **5** possesses eight H-bonds [figure 4(b)] linking the adjacent four molecules into a 2-D wavelike structure [figure 4(c)]. If the molecule can be seen as a 4-connected node, the sheet could be simplified to *sq1* topology with a point symbol of $(4^4{\cdot}6^2)$ [figure 4(d)].

3.2. *PXRD and TGA studies*

In order to characterize the phase purity of other crystalline materials, PXRD patterns for **1–5** were performed at room temperature (figure S2). The location and intensity of diffraction peaks of calculated and experimental patterns match well, indicating that these complexes were synthesized as a single phase.

Thermogravimetric experiments of **1–5** were carried out in the atmosphere from 30 to 800 °C. The TGA curves of **1–5** are shown in figure S3. The TG curve of **1** suggests that **1** exhibits four main steps of weight losses. The first weight loss is at 104–166 °C, corresponding to loss of two lattice water molecules and two coordinated waters (found 14.75%, Calcd 15.08%). The second step of weight loss from 166 to 320 °C corresponds to the removal of carboxyl from one L^1 (found 9.06%, Calcd 9.21%). The third step of 320–495 °C is consistent with decomposition of the decarboxylated L^1 (found 28.59%, Calcd 27.23%). The fourth step of 30.16% from 495 to 585 °C can be attributed to decomposition of the other L^1 (Calcd 32.89%). In short, two HL^1 ligands are lost in a continuous fashion from 166 to 585 °C (found 67.93%, Calcd 69.13%) with residue of CoO (found 15.42%, Calcd 15.69%). Complex **2** loses its lattice and coordinated waters from 108 to 162 °C (found 12.59%, Calcd 13.56%). The mass loss of 27.60% between 162 and 366 °C can be attributed to loss of L^1 (Calcd 29.57%), then the decomposition of the other L^1 occurred from 366 to 538 °C (found 30.27%, Calcd 32.60%) with the residue of CdO (found 25.57%, Calcd 24.11%). Complexes **3** and **4** are isomorphic with similar TG curves. The first weight loss could be ascribed to loss of three coordinated waters (108–160 °C, found 14.93%, Calcd 15.73% for **3**, 112–183 °C, found 14.62%, Calcd 15.74% for **4**). The second weight loss may correspond to loss of two carboxyl groups (160–358 °C, found 23.32%, Calcd 25.64% for **3**, 183–354 °C, found 27.89%, Calcd 25.66% for **4**). The third and the fourth weight losses are equivalent to loss of the other residues of L^2 (358–541 °C, found 39.36%, Calcd 41.96% for **3**, and 354–519 °C, found 39.14%, Calcd 41.98% for **4**). The remaining weight can be ascribed to CoO for **3** (found 23.58%, Calcd 21.83%) and NiO for **4** (found 21.07%, Calcd 21.78%). Complex **5** exhibits three weight loss stages. The first 5.89% (Calcd 5.77%) from 54 to 174 °C corresponds to loss of two coordinated waters. The second and the third stage, occurring between 174 and 530 °C (found 80.21%, Calcd 81.40%) are equivalent to decomposition of two H_2L^2 ligands with residue of CuO (found 12.52%, Calcd 12.83%).

3.3. *Effect of different processes on decolorization of MO*

In order to investigate the effect of these complexes on dye decolorization, MO solutions were exposed under six different processes: (a) direct photolysis under solar light irradiation; (b) 10 drops of hydrogen peroxide under solar light irradiation; (c) complex **3**-H_2O_2 system under solar light irradiation; (d) complex **3** under solar light irradiation; (e) H_2L^2-H_2O_2 system under solar light irradiation; (f) $CoCl_2$-H_2O_2 system under solar light irradiation. The results are shown in figure 5. Obviously, almost no decolorization of MO solution was observed in a, b, e, and f. The removal rate of MO solution was about 37.5% after 17 h in process (d) when complex **3** acted as catalyst [figure 5(d)]. Interestingly, about 80.7% of MO was decolorized after 17 h in the case of 0.058 mmol of **3** in the presence of H_2O_2 [figure 5(c)]. The results imply that **3** has visible light photocatalytic activity for decolorization of MO at atmospheric conditions, while, when H_2O_2 was utilized as oxidant [30, 31], the catalytic efficiency is significantly improved.

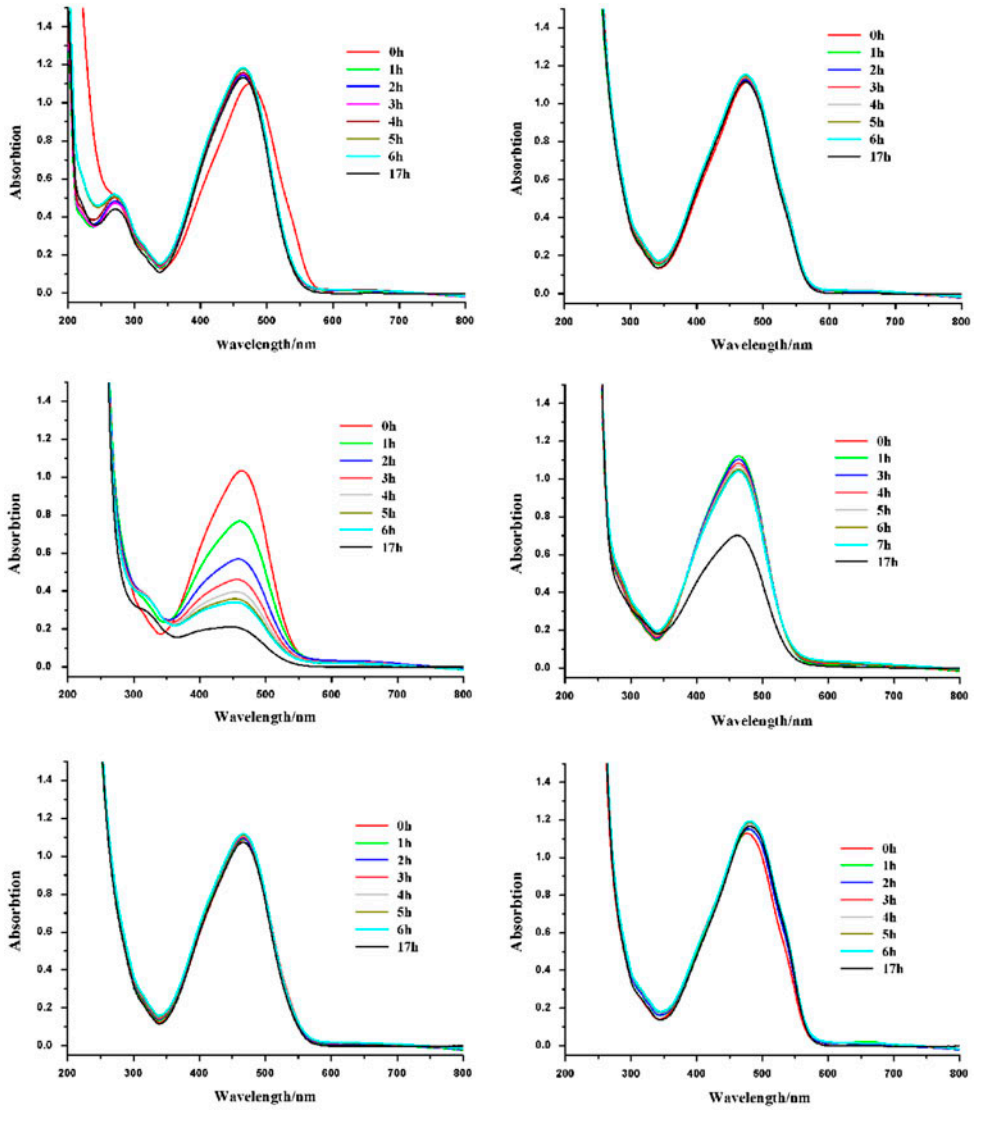

Figure 5. UV–vis spectra of the different processes for decolorization of MO in aqueous solution: (a) direct photolysis under solar light irradiation; (b) 10 drops of hydrogen peroxide under solar light irradiation; (c) **3**-H_2O_2 system under solar light irradiation; (d) **3** as catalyst under solar light irradiation; (e) catalytic decolorization by H_2L^2-H_2O_2 system under solar light irradiation; (f) $CoCl_2$-H_2O_2 system under solar light irradiation. Experimental conditions: $[MO]_0$ = 15 mg·L^{-1}; C_{H2O2} = 30%; initial pH 5.8; $N_{(Catalyst)}$ = 0.058 mmol.

3.4. *Anticancer activities*

In 1970s, Rosenberg found that platinum compounds have anticancer activity, which opened up a new direction for cancer drug research as a new class of potent antitumor agents [32]. Considering the biologically active triazole groups in HL^1 and H_2L^2 [33–36], the cytotoxicity tests of this series of complexes were carried out. The cytotoxicity tests for

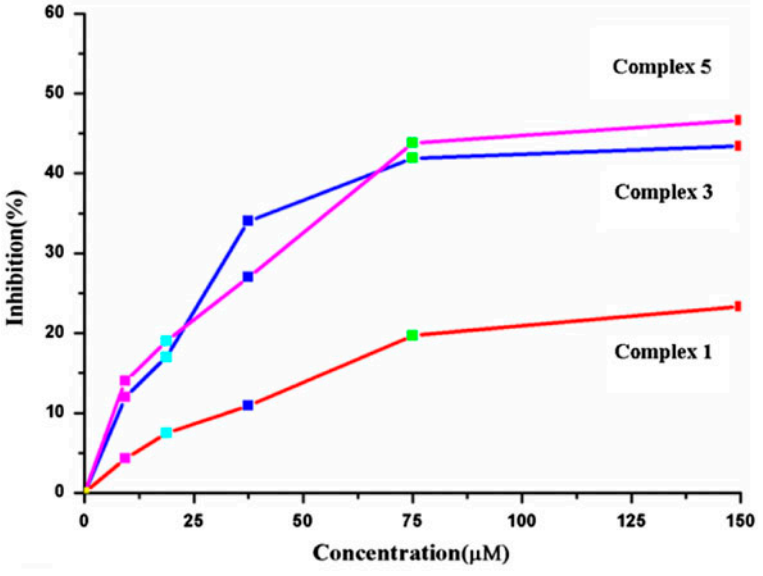

Figure 6. Results of MTT assay of **1**, **3**, and **5** on HepG2 cells at concentration ranging from 0 to 150 μM.

1, **3**, and **5** were assessed by the MTT assay. The HepG2 cells were incubated in the presence of **1**, **3**, and **5** in different concentrations for 24 h.

The assay was performed in triplicate, and the results of MTT assay on HepG2 cells with complexes concentration ranging from 0 to 150 μM are shown in figure 6. Complexes **1**, **3**, and **5** showed obvious inhibitory activities on HepG2 cells under tested concentrations for 24 h. The HepG2 cell inhibition rate increased with increasing concentrations of **1**, **3**, and **5**. Complexes **3** and **5** exhibit much better inhibitory activities than **1**. More than 40% of HepG2 cells could be inhibited in the presence of 75 μM of **3** or **5**.

4. Conclusion

Five complexes based on N-heterocyclic carboxylate ligands HL^1 or H_2L^2 and transition metals have been hydrothermally/solvothermally synthesized. The remarkable feature of the structure of this series of complexes is the existence of many H-bonds. It can be attributed to both HL^1 and H_2L^2 having multiple H-bonds donor and acceptor groups as well as the existence of water molecules. There are nine H-bonds in **1**, seventeen H-bonds in **2**, ten H-bonds in **3** and **4**, and eight H-bonds in **5**. In these five complexes, the intermolecular H-bonds drive the building blocks to form 3-D or 2-D supramolecular architectures with complicated topologies. **3** shows good visible light photocatalytic activity for the decolorization of MO at atmospheric conditions. Complexes **1**, **3**, and **5** have obvious anticancer activities for inhibiting the growth of HepG2 cells.

Supplementary material

Electronic Supplementary Information (ESI) available: X-ray crystallographic files in CIF format, table of selected bond lengths and bond angles, hydrogen bonds lengths and angles, FT-IR and PXRD spectra and TGA curves. See doi: 10.1039/b000000x/.

Disclosure statement

No potential conflict of interest was reported by the authors.

Funding

This work was financially supported by the National Natural Science Foundation of China [grant number 21371052]; Heilongjiang Province Science and Technology Project [grant number GZ13A002].

References

[1] (a) O.M. Yaghi, H. Li, C. Davis, D. Richardson, T.L. Groy. *Acc. Chem. Res.*, **31**, 474 (1998); (b) M. Eddaoudi, D.B. Moler, H. Li, B. Chen, T.M. Reineke, M. O'Keeffe, O.M. Yaghi. *Acc. Chem. Res.*, **34**, 319 (2001); (c) B. Moulton, M.J. Zaworotko. *Chem. Rev.*, **101**, 1629 (2001); (d) C.N.R. Rao, S. Natarajan, R. Vaidhyanthan. *Angew. Chem., Int. Ed.*, **43**, 1466 (2004); (e) S. Kitagawa, R. Kitaura, S. Noro. *Angew. Chem., Int. Ed.*, **43**, 2334 (2004); (f) S. Kitagawa, K. Uemura. *Chem. Soc. Rev.*, **34**, 109 (2005); (g) S. Horike, R. Matsuda, D. Tanaka, M. Mizuno, K. Endo, S. Kitagawa. *J. Am. Chem. Soc.*, **128**, 4222 (2006).

[2] (a) M.J. Manos, R. Iyer, E. Quarez, J.H. Liao, M.G. Kanatzidis. *Angew. Chem., Int. Ed.*, **44**, 3552 (2005); (b) P.N. Trikalitis, K.K. Rangan, T. Bakas, M.G. Kanatzidis. *J. Am. Chem. Soc.*, **124**, 12255 (2002); (c) M. Latroche, S. Surble, C. Serre, C. Mellot-Draznieks, P.L. Llewellyn, J.H. Lee, J.S. Chang, S.H. Jhung, G. Ferey. *Angew. Chem., Int. Ed.*, **45**, 8227 (2006); (d) D.F. Sun, S.Q. Ma, Y.X. Ke, D.J. Collins, H.C. Zhou. *J. Am. Chem. Soc.*, **128**, 3896 (2006); (e) S. Surble, F. Millange, C. Serre, T. Duren, M. Latroche, S. Bourrelly, P.L. Llewellyn, G. Ferey. *J. Am. Chem. Soc.*, **128**, 14889 (2006).

[3] (a) X. Lin, A.J. Blake, C. Wilson, X.Z. Sun, N.R. Champness. *J. Am. Chem. Soc.*, **128**, 10745 (2006); (b) L. Pan, D.H. Olson, L.R. Ciemnolonski, R. Heddy, J. Li. *Angew. Chem., Int. Ed.*, **45**, 616 (2006).(c) C.D. Wu, W.B. Lin. *Angew. Chem., Int. Ed.*, **46**, 1075 (2007); (d) M. Yoshizawa, T. Kusukawa, M. Kawano, T. Ohhara, I. Tanaka, K. Kurihara, N. Niimura, M. Fujita. *J. Am. Chem. Soc.*, **127**, 2798 (2005); (e) Q. Yu, X.L. Sun, X.Q. Zhang, F.P. Huang, H.D. Bian, H. Liang. *J. Coord. Chem.*, **64**, 3609 (2011).

[4] Z.G. Gu, Y.T. Liu, X.J. Hong, Q.G. Zhan, Z.P. Zheng, S.R. Zheng, W.S. Li, S.J. Hu, Y.P. Cai. *Cryst. Growth Des.*, **12**, 2178 (2012).

[5] H. Zhao, J.M. Chen, J.R. Lin, W.X. Wang. *J. Coord. Chem.*, **64**, 2735 (2011).

[6] S.Q. Zhang, F.L. Jiang, M.Y. Wu, R. Feng, J. Ma, W.T. Xu, M.C. Hong. *Inorg. Chem. Commun.*, **14**, 1400 (2011).

[7] B. Zhao, X.Y. Chen, P. Cheng, D.Z. Liao, S.P. Yan, Z.H. Jiang. *J. Am. Chem. Soc.*, **126**, 15394 (2004).

[8] L.R. Yang, S. Song, C.Y. Shao, W. Zhang, H.M. Zhang, Z.W. Bu, T.G. Ren. *Synth. Met.*, **161**, 1500 (2011).

[9] L.R. Yang, S. Song, H.M. Zhang, W. Zhang, Z.W. Bu, T.G. Ren. *Synth. Met.*, **161**, 2230 (2011).

[10] L.R. Yang, S. Song, C.Y. Shao, W. Zhang, H.M. Zhang, Z.W. Bu, T.G. Ren. *Synth. Met.*, **161**, 925 (2011).

[11] L. Chen, X.M. Lin, Y. Ying, Q.G. Zhan, Z.H. Hong, J.Y. Li, N.S. Weng, Y.P. Cai. *Inorg. Chem. Commun.*, **12**, 761 (2009).

[12] Z.Q. Xia, Q. Wei, S.P. Chen, X.M. Feng, G. Xie, C.F. Qiao, G.C. Zhang, S.L. Gao. *J. Solid State Chem.*, **197**, 489 (2013).

[13] X.D. Chen, H.F. Wu, X.H. Zhao, M. Du. *Cryst. Growth Des.*, **7**, 124 (2007).

[14] L.X. Xie, X.W. Hou, Y.T. Fan, H.W. Hou. *Cryst. Growth Des.*, **12**, 1282 (2012).

[15] J.M. Xu, E. Zhang, X.J. Shi, Y.C. Wang, B. Yu, W.W. Jiao, Y.Z. Guo, H.M. Liu. *Eur. J. Med. Chem.*, **80**, 593 (2014).

[16] L. Qin, D.Y. Ma, R. Deng, J. Xu. *J. Coord. Chem.*, **67**, 1032 (2014).

[17] I. Khan, S. Zaib, A. Ibrar, N.H. Rama, J. Simpson, J. Iqbal. *Eur. J. Med. Chem.*, **78**, 167 (2014).

[18] G.B. Bagihalli, P.G. Avaji, S.A. Patil, P.S. Badami. *Eur. J. Med. Chem.*, **43**, 2639 (2008).

[19] R. Luebke, J.F. Eubank, A.J. Cairns, Y. Belmabkhout, L. Wojtas, M. Eddaoudi. *Chem. Commun.*, **48**, 1455 (2012).

[20] S.S. Xiong, Y.B. He, R. Krishna, B.L. Chen, Z.Y. Wang. *Cryst. Growth Des.*, **13**, 2670 (2013).

[21] B. Liu, R.L. Zhao, K.F. Yue, J.T. Shi, Y. Yu, Y.Y. Wang. *Dalton Trans.*, **42**, 13990 (2013).
[22] M. Du, Z.H. Zhang, Y.P. You, X.J. Zhao. *CrystEngComm*, **10**, 306 (2008).
[23] Y. Hou, T.A. Zhao, P. Okamura, W.Y. Wang. *Sun. J. Coord. Chem.*, **65**, 4409 (2012).
[24] G.R. Desiraju. *Angew. Chem., Int. Ed. Engl.*, **34**, 2311 (1995).
[25] G.R. Desiraju. *Crystal Engineering-The Design of Organic Solids*, Elsevier, Amsterdam (1989).
[26] M. Tabatabaee, S. Rashidi, M. Islaminia, M. Ghassemzadeh, K. Molčanov, B. Neumüller. *J. Coord. Chem.*, **65**, 3499 (2012).
[27] J. Thomas-Gipson, G. Beobide, O. Castillo, M. Früba, F. Hoffmann, A. Luque, S. Pérez-Yánez, P. Román. *Cryst. Growth Des.*, **14**, 4019 (2014).
[28] G.M. Sheldrick. *Acta Crystallogr., Sect. A*, **64**, 112 (2008).
[29] V.A. Blatov, A.P. Shevchenko, D.M. Proserpio. *Cryst. Growth Des.*, **14**, 3576 (2014).
[30] M. Ge, L. Liu, W. Chen, Z. Zhou. *CrystEngComm*, **14**, 1038 (2012).
[31] G.H. Cui, C.H. He, C.H. Jiao, J.C. Geng, V.A. Blatov. *CrystEngComm*, **14**, 4210 (2012).
[32] B. Rosenberg, L. VanCamp, J.E. Trosko, V. Manosour. *Nature*, **222**, 385 (1969).
[33] I. Bratsos, D. Urankar, E. Zangrando, P. Genova-Kalou, J. Košmrlj, E. Alessio, I. Turel. *Dalton Trans.*, **40**, 5188 (2011).
[34] M. Delferro, L. Marchiò, M. Tegoni, S. Tardito, R. Franchi-Gazzola, M. Lanfranchi. *Dalton Trans.*, **38**, 3766 (2009).
[35] B.B. Xu, P. Shi, Q.Y. Guan, X. Shi, G.L. Zhao. *J. Coord. Chem.*, **66**, 2605 (2013).
[36] K.K.W. Lo, M.W. Louie, K.S. Sze, J.S.Y. Lau. *Inorg. Chem.*, **47**, 602 (2008).